Ordered State in a Haldane Material $PbNi_2V_2O_8$ Doped with Magnetic and Non-Magnetic Impurities

S. Imai,* T. Masuda,† T. Matsuoka,‡ and K. Uchinokura§
Department of Advanced Materials Science, The University of Tokyo, 5-1-5 Kashiwa-no-ha, Kashiwa 277-8581, Japan
(Dated: February 2, 2008)

Impurity effect is systematically studied in doped Haldane material $Pb(Ni_{1-x}M_x)_2V_2O_8$ (M = Mn, Co, Cu, and Mg) by use of DC and AC susceptibility, and heat capacity measurements. The occurrence of three-dimensional ordered state is universally observed for all the impurities and the complete temperature – concentration phase diagrams are obtained, which are qualitatively similar to that in other spin-gap materials. The unique feature is found in the drastic dependence of the transition temperatures on the species of the impurities. The consideration of effective Hamiltonian based on VBS model makes it clear that the ferromagnetic next-nearest-neighbor interaction and the antiferromagnetic nearest-neighbor interaction between impurity and edge spins play a key role in the unique feature.

I. INTRODUCTION

Low-dimensional quantum magnetism is one of the most exciting topics in condensed matter physics. The simplest model is realized in one-dimensional Heisenberg antiferromagnet, where the Hamiltonian is expressed as

$$\mathcal{H} = J\sum_j \boldsymbol{S}_j \cdot \boldsymbol{S}_{j+1}, \qquad J > 0. \tag{1}$$

Exact ground state in $S = 1/2$ is non-magnetic singlet[1] and its excitation is gapless known as des Cloizeaux-Pearson mode.[2] In 1983 Haldane pointed out a qualitative difference between spin integer and half integer in Eq. (1); in the former spin correlation decays exponentially and spin excitation has a spin gap, while in the latter the correlation decays by power law and the excitation is gapless.[3,4] A mimic model of spin integer Heisenberg antiferromagnetic chain known as AKLT (Affleck, Kennedy, Lieb, and Tasaki) Hamiltonian[5,6] was proposed by adding a quadratic term in Eq. (1). AKLT Hamiltonian can be solved analytically and the ground state, which is known as valence-bond-solid (VBS) state, is similar to that of simple Heisenberg Hamiltonian. In a finite chain staggered spins are induced in the vicinity of its edges[5,6] and they can be approximated as a couple of effective $S = 1/2$ spins on edges. Edge spins predicted by AKLT Hamiltonian is realized in the impurity-doped Haldane chain, as is schematized in Fig. 1 (a), and the low energy excitation can be expressed by the effective Hamiltonian consisting of three spins with open boundary condition;

$$\mathcal{H} = J_M(\boldsymbol{s}_1 \cdot \boldsymbol{S}_M + \boldsymbol{S}_M \cdot \boldsymbol{s}_2). \tag{2}$$

The predicted energy excitations were observed in the ESR spectrum in impurity-doped Haldane material NENP (Ref. 7) and numerical calculation also supports application of AKLT Hamiltonian to Haldane chain.[8,9]

$PbNi_2V_2O_8$ is a new member of inorganic Haldane materials discovered by Uchiyama *et al.* in 1999.[10] The Haldane gap was confirmed by the bulk susceptibility, high-field magnetization, and inelastic neutron scattering.[10,11] The unique feature in $PbNi_2V_2O_8$ is spin-vacancy-induced antiferromagnetic phase in $Pb(Ni_{1-x}Mg_x)_2V_2O_8$,[10,12] where coexistence of gapless and gap excitations is suggested. The occurrence of the antiferromagnetic phase is attributed to the *ferromagnetic next-nearest-neighbor interaction* and the *in-*

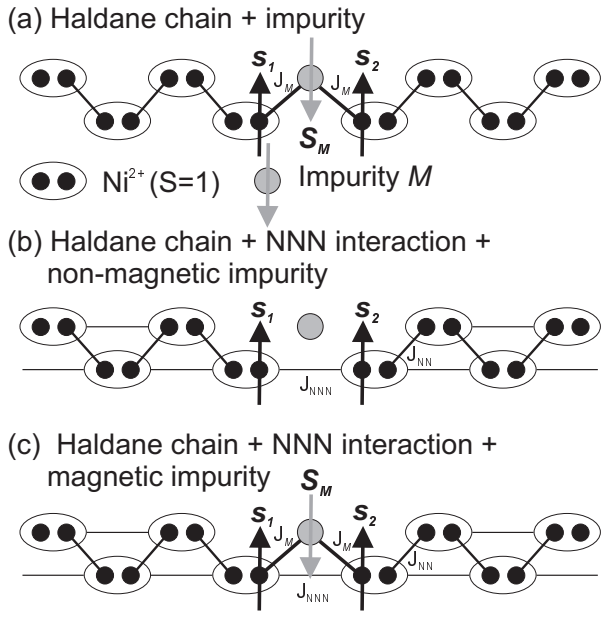

FIG. 1: (a) Effective spin configuration in doped-Haldane chain. $S = 1$ spins are described by a couple of $S = 1/2$ spins (filled circles), and symmetrization operator (ellipsoids). Adjacent $S = 1/2$ spins on different Ni^{2+} sites are coupled by singlet bond (solid line). (b) Effective spin configuration in non-magnetic impurity doped Haldane chain with next-nearest-neighbor interaction. The next-nearest-neighbor interaction $J_{\rm NNN}$ and nearest-neighbor interaction $J_{\rm NN}$ is indicated by thin and bold solid lines, respectively. (c) Effective spin configuration in magnetic impurity doped Haldane chain with next-nearest-neighbor interaction.

terchain interaction. The former is indicated by powder neutron scattering[13] and ESR[14] measurements and decisively confirmed by the consideration of Schottky heat capacity.[15] The latter is confirmed by careful analysis of powder neutron scattering measurements.[11] In the antiferromagnetic long-range-ordered state, spins adjacent to impurity must be parallel as is schematized in Fig. 1 (b). Therefore, ferromagnetic next-nearest-neighbor interaction favors antiferromagnetic ordering. Interchain interaction is, of course, necessary for the three-dimensional ordering due to Mermin-Wagner theorem.[16]

Since the low energy excitation in doped NENP was well described by the effective Hamiltonian Eq. (2), a similar approach could be useful to understand the ordered state of doped $PbNi_2V_2O_8$. Effective Hamiltonian for Mg^{2+} ($S = 0$)-doped $PbNi_2V_2O_8$ will be

$$\mathcal{H}_1 = J_{\rm NNN}\boldsymbol{s}_1 \cdot \boldsymbol{s}_2, \qquad J_{\rm NNN} < 0, \tag{3}$$

which is actually the Hamiltonian for ferromagnetic dimer. The ground state is $S = 1$ triplet states, where the spins are parallel to each other, and favors three-dimensional ordering. On the other hand the effective Hamiltonian for $PbNi_2V_2O_8$ doped with a magnetic impurity is expressed as three spin ring as is shown in Fig. 1 (c);

$$\mathcal{H}_2 = J_M(\boldsymbol{s}_1 \cdot \boldsymbol{S}_M + \boldsymbol{S}_M \cdot \boldsymbol{s}_2) + J_{\rm NNN}\boldsymbol{s}_1 \cdot \boldsymbol{s}_2. \tag{4}$$

In this case the ground state depends on the sign of J_M and also the type of spin interaction such as Heisenberg, Ising, and XY. Because they are subject to the species of impurity ions M, systematic study on doped $PbNi_2V_2O_8$ may be valuable to reveal the nature of the interaction among the impurity spins and edge spins. Although there have been several studies in nonmagnetic impurity-doped $PbNi_2V_2O_8$,[10,12,14,15,17] study of magnetic-impurity doped $PbNi_2V_2O_8$ is very rare and even preliminary.[18] We will report a complete study in $Pb(Ni_{1-x}M_x)_2V_2O_8$ (M = Mn, Co, Cu, and Mg) and have found the drastic dependence on the kind of impurities in the temperature – concentration (T–x) phase diagram.

To study the magnetic excitations neutron inelastic scattering would be the most effective tool if a single crystal of reasonable size were available. However, $PbNi_2V_2O_8$ is incongruent and it is hard to obtain large single crystal. Therefore the best we can do is bulk measurements such as magnetic susceptibility and heat capacity on polycrystalline samples. Experimental details will be briefly mentioned in section II. In section III A and C the value and number of effective spins induced by impurities are carefully discussed and the sign of J_M are obtained. The value of effective spin is estimated to be $|S_M - 1|$ in $Pb(Ni_{1-x}M_x)_2V_2O_8$ (M = Mn, Co, and Cu) and J_M is proved to be antiferromagnetic. In section III B antiferromagntic transition is confirmed in $Pb(Ni_{1-x}Cu_x)_2V_2O_8$ at extremely low temperatures. In section III D the T–x phase diagrams are obtained in $Pb(Ni_{1-x}M_x)_2V_2O_8$ (M = Mn, Co, Mg, and Cu). In section IV the weak ferromagnetism in $Pb(Ni_{1-x}Co_x)_2V_2O_8$, the drastic dependence of the transition temperatures on the species of the impurities in T–x phase diagram, and the comparison with impurity-doped spin-Peierls material $CuGeO_3$ are discussed.

II. EXPERIMENTAL DETAILS

Polycrystalline samples of $Pb(Ni_{1-x}M_x)_2V_2O_8$ (M = Mn, Co, Mg, and Cu) were prepared by solid state reaction method. Aligned samples were prepared by applying magnetic field to the mixture of powder sample and epoxy resin (Stycast 1266) at room temperature.[10] DC magnetic susceptibilities were measured down to 2.0 K in $H = 0.1$ T magnetic field by SQUID magnetometer (MPMS-XL of Quantum Design Corp.) AC susceptibilities were measured down to 50 mK in zero static magnetic field by using an adiabatic demagnetization refrigerator (μFridge of Cambridge Magnetic Refrigeration Corp.). Heat capacities were measured down to 0.4 K by the relaxation method (PPMS with Helium-3 option of Quantum Design Corp.) in a magnetic field up to 12 T.

III. EXPERIMENTAL RESULTS

A. DC Magnetic Susceptibility

Figure 2 shows that a magnetic anomaly is detected in the DC magnetic susceptibility in $Pb(Ni_{1-x}Mn_x)_2V_2O_8$ ($x = 0.050$) aligned sample. A sharp peak in $\boldsymbol{H} \parallel c$ axis and a slight anomaly in $\boldsymbol{H} \perp c$ at 2.3 K in the inset of Fig. 2 confirms that the ground state is an easy-axis type antiferromagnetic long-range order. The phase transition is observed also in the polycrystalline sample of $x = 0.030$. No anomaly in the lower concentration sample $x = 0.010$ is simply because of our experimental limit.

Figure 3 shows the temperature dependence of the magnetic susceptibilities in $Pb(Ni_{1-x}Co_x)_2V_2O_8$. They were measured both in a field cooling (FC) and in a zero-field cooling (ZFC) processes. The impurity-induced anomalies are observed at $T = 2.2$ K for $x = 0.010$ and $T = 4.2$ K for $x = 0.020$, and the hysteresis between FC and ZFC were detected below the anomaly's temperature. The magnetic susceptibilities seem to have a finite values for both processes at $T = 0$ K, which would be attributed to an antiferromagnetic transition with weak spontaneous magnetization. In mixed spin materials spin glass is another possibility but the jump in the heat capacity, which we will see later, prefers weak ferromagnetism. The weak ferromagnetism is possible owing to the existence of the Dzyaloshinskii-Moriya antisymmetric interaction[19,20] as will be discussed in the section IV.

No anomalies are detected in any concentration samples of $Pb(Ni_{1-x}Cu_x)_2V_2O_8$ in the measurements down

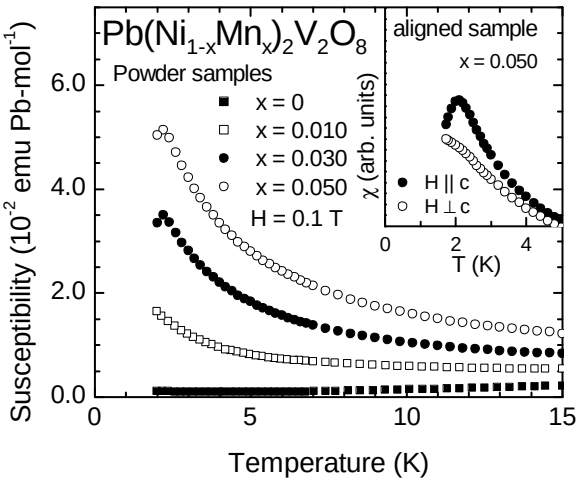

FIG. 2: Temperature dependence of the magnetic susceptibilities in $Pb(Ni_{1-x}Mn_x)_2V_2O_8$. Inset shows the anisotropy of the aligned polycrystalline sample with $x = 0.050$.

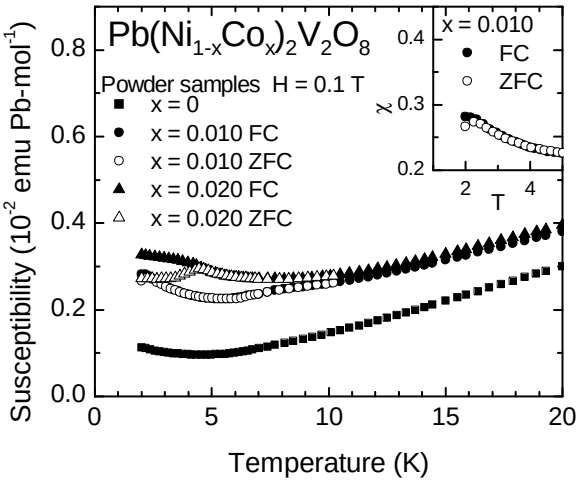

FIG. 3: Temperature dependence of the magnetic susceptibilities in $Pb(Ni_{1-x}Co_x)_2V_2O_8$. The inset is the low temperature susceptibility in $x = 0.01$ sample.

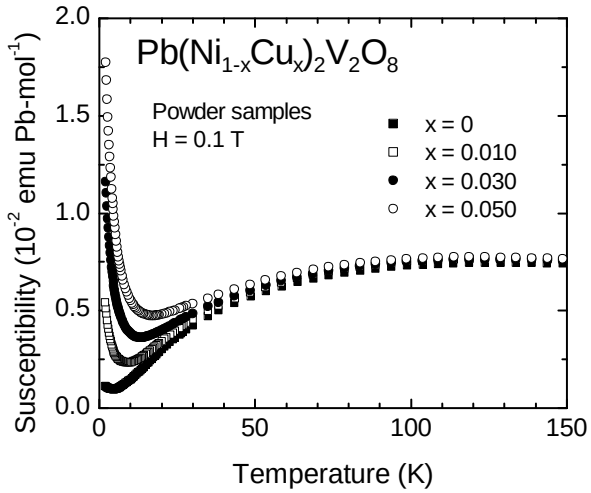

FIG. 4: Temperature dependence of the magnetic susceptibilities in $Pb(Ni_{1-x}Cu_x)_2V_2O_8$.

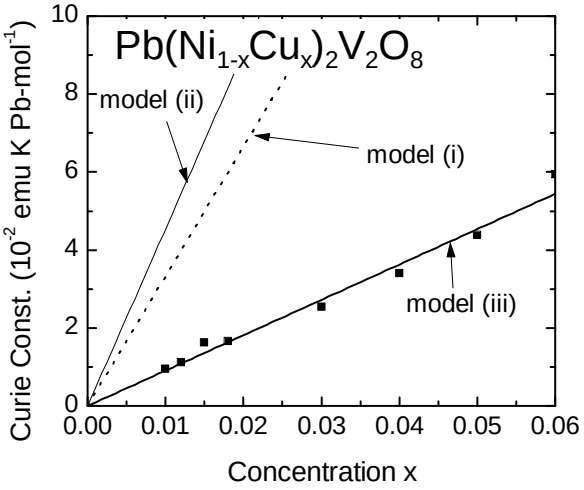

FIG. 5: Curie constants of $Pb(Ni_{1-x}Cu_x)_2V_2O_8$ from the measurement of the magnetic susceptibility and the calculated values from the three models.

to $T = 2$ K. In contrast with other impurities Cu-doping only enhances Curie-like susceptibility at low temperatures which is shown in Fig. 4.

Hereafter we will estimate the number and the value of impurity-induced effective spins based on VBS model, where the magnetization in a finite chain is presumed to be induced only by the edge spins.[5,6] Let us assume that the susceptibility is expressed as a sum of the two contributions in the low impurity concentration region:

$$\chi = \chi_{\rm pure} + \chi_{\rm para}, \tag{5}$$

where $\chi_{\rm pure}$ is the susceptibility in pure $PbNi_2V_2O_8$ and $\chi_{\rm para}$ is the additional susceptibility due to impurity-induced spins. If $\chi_{\rm para}$ obeys Curie-Weiss law, the number and the value of the impurity-induced-effective spins will be obtained from Curie constants. As was already mentioned in the introduction the *ferromagnetic next-nearest-neighbor interaction* exists, which is in fact confirmed by the observation of effective spin with $S = 1$ in $Pb(Ni_{1-x}Mg_x)_2V_2O_8$ by some of the present authors.[15] Therefore, the following three models are possible in impurity-doped $PbNi_2V_2O_8$;

(i) The interaction between the edge spin and the impurity spin, J_M in Eq. (4), is very small and edge spins are coupled by ferromagnetic next-nearest-neighbor interaction. One effective spin with $S =$

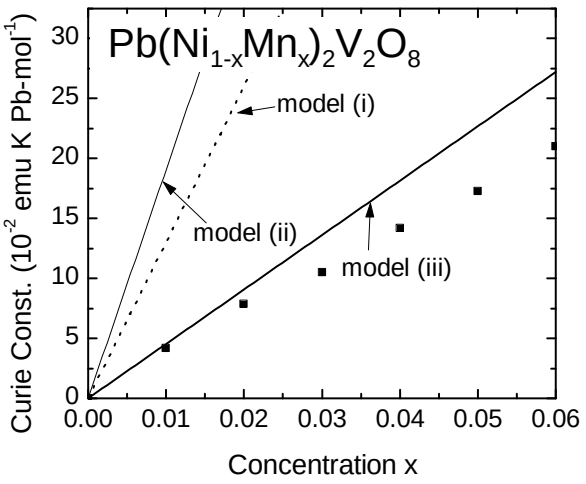

FIG. 6: Curie constants of $Pb(Ni_{1-x}Mn_x)_2V_2O_8$ from the measurement of the magnetic susceptibility and the calculated values from the three models.

1 and one with $S = S_M$ will be detected.

(ii) J_M is ferromagnetic and one effective spin with $S = S_M + 1$ will be detected.

(iii) J_M is antiferromagnetic and one effective spin with $S = |S_M - 1|$ will be detected.

Curie constants of $Pb(Ni_{1-x}Cu_x)_2V_2O_8$ are plotted as a function of x in Fig. 5. Three lines are calculated values from the above three models. The experimental data are close to the theoretical line of the model (iii) and this suggests that $J_{\rm Cu}$ in Eq. (4) is antiferromagnetic.

In the same way $\chi_{\rm para}$ of $Pb(Ni_{1-x}Mn_x)_2V_2O_8$ were fitted by the Curie-Weiss law and the experimental Curie constants and the calculated values of the three models are plotted in Fig. 6. The same argument on $Pb(Ni_{1-x}Cu_x)_2V_2O_8$ may lead to the conclusion that the most suitable theoretical value is the model (iii), at least for $x \to 0$. Hence the impurity-induced spins have $S = 3/2$ degree of freedom at each impurity site and $J_{\rm Mn}$ is antiferromagnetic.

We assumed $g = 2.2$ implicitly because Zorko *et al.*[14] has shown that the broad ESR resonance has $g \sim 2.2$ between room temperature and 70 K for $Pb(Ni_{1-x}Mg_x)_2V_2O_8$ ($x \leq 0.24$). However, we have to be careful about it because the ESR resonance was attributed to the bulk spins (on Ni^{2+} ions) and not that on impurity ions. At low temperatures they observed the shift of the resonance line, which can be due to the growing contribution of impurity-related resonance.[14] Therefore it might be difficult to definitely determine which of the three models is the best description of the spin state only by the susceptibility measurement. Since magnetic entropy also gives information on the value and the number of spins and it is independent on g value, heat-capacity measurements might be more useful to discuss the model precisely. We will see that our argument here is consistent with heat capacity measurements in III C.

B. AC Susceptibility at Very Low Temperatures

Although the DC magnetic susceptibility and heat capacity in $Pb(Ni_{1-x}Cu_x)_2V_2O_8$ have been measured down to 2 K in the same way as the samples doped with other species of impurities, three-dimensional ordering has not been found yet[18] (see also III A). There arizes a question if there is no transition in $Pb(Ni_{1-x}Cu_x)_2V_2O_8$ or the transition temperature is extremely low. To search for the magnetic phase transition in $Pb(Ni_{1-x}Cu_x)_2V_2O_8$, measurements of AC susceptibility at low temperatures (down to 50 mK) were performed using the adiabatic demagnetization method. The real parts of the AC susceptibilities in $Pb(Ni_{1-x}Cu_x)_2V_2O_8$ at very low temperatures are shown in Fig. 7; here the absolute value was not exactly obtained because of the specification of the AC susceptibility method but it is sufficient to determine the existence or absence of the transition and also to determine the transition temperature if it exists. The external static magnetic field was not applied in this experiment.

For the sample with $x = 0.010$, the change of the susceptibility is likely to follow the Curie-Weiss law and no anomaly was found above 50 mK. For the sample with $x = 0.020$, however, an anomaly appears in the susceptibility-temperature curve at $\sim$ 0.2 K and the susceptibility-temperature curve becomes flat below this temperature. For the samples with $x \geq 0.30$ we observed a distinct peak in the susceptibility-temperature curve and the peak temperature increases with the impurity (Cu^{2+}) concentration.

This behavior is qualitatively the same as that of $Pb(Ni_{1-x}Mg_x)_2V_2O_8$, which has three-dimensional ordering at low temperatures, and we attributed the peaks in $Pb(Ni_{1-x}Cu_x)_2V_2O_8$ to magnetic orderings. Hence, we concluded that the ground state of $Pb(Ni_{1-x}Cu_x)_2V_2O_8$ is also the ordered state as the samples doped with other impurities. However, temperature scale of the ordering temperature is quite different. This will be discussed in section IV.

C. Heat Capacity

We obtained the magnetic heat capacity $C_{\rm m}$ by subtracting the heat capacity of $PbMg_2V_2O_8$, which is isostructural to $PbNi_2V_2O_8$ from that of $Pb(Ni_{1-x}M_x)_2V_2O_8$. The magnetic entropy $S_{\rm m}$ was obtained according to the equation $S_{\rm m} = \int_0^T \frac{C_{\rm m}}{T} dT$. Figure 8 shows the magnetic heat capacity (upper panel) and magnetic entropy (lower panel) of $Pb(Ni_{1-x}Cu_x)_2V_2O_8$ with $x = 0.050$. For $H = 0$ T a small anomaly is observed at $\sim$ 0.5 K, which is probably attributed to the antiferromagnetic ordering because the temperature is

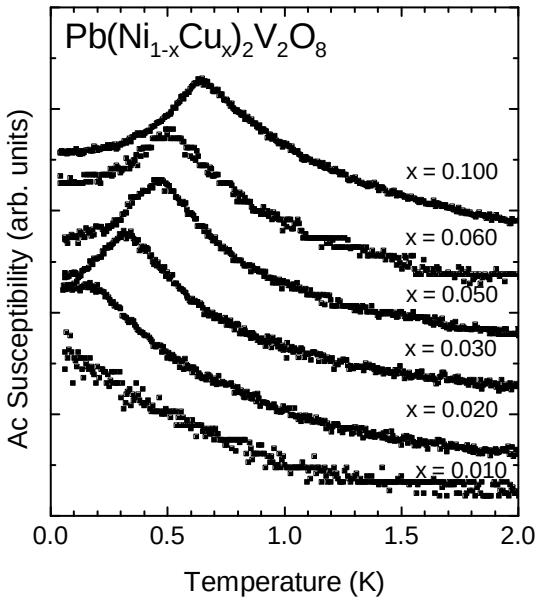

FIG. 7: Temperature dependence of the AC susceptibilities in $Pb(Ni_{1-x}Cu_x)_2V_2O_8$ at very low temperatures.

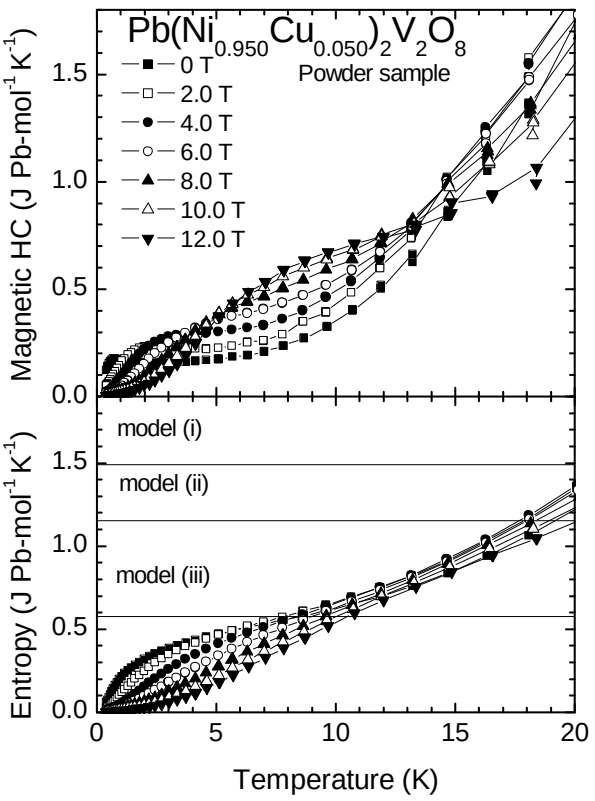

FIG. 8: Magnetic heat capacity (upper panel) and magnetic entropy (lower panel) of $Pb(Ni_{1-x}Cu_x)_2V_2O_8$ with $x = 0.050$.

close to the peak temperature, 0.46 K, in the AC susceptibility. This anomaly diminishes by the application of a magnetic field. This is the typical behavior of classical antiferromagnetic transition. In magnetic field there appears a Schottky-like broad anomaly at higher temperature and the anomaly's temperature increases with the magnetic field. This behavior was already reported in $Pb(Ni_{1-x}Mg_x)_2V_2O_8$ (Ref. 15) and the difference is the energy scale of the ordered state such as the transition temperature or the critical field for the disappearance of the ordered state.

If we assume that the system can be approximated by an assembly of the free spins (effective spins) of the same S value, the entropy of the system will be saturated at $S_{\rm m} = Nk_{\rm B}\ln(2S+1)$. Note that the above expression does not contain the g value. Therefore the magnetic entropy would be more appropriate quantity to obtain the value and the number of spins than the Curie constant. The saturation values of the three models which is described in section III A are shown in the lower panel of Fig. 8 (solid lines). We can see that the entropies at the various values of the magnetic fields converge to almost the same values at $T \sim 12$ K and a point of inflection seems to exist there.

In addition to the induced moments as effective spins, there exist other contributions to magnetic entropy.

(a) One is the contribution from the spin-gap excitation. Haldane-like gap excitation, in which the energy scale is about 20 K, was observed in $Pb(Ni_{1-x}Mg_x)_2V_2O_8$ by the high field magnetization measurement[15] and coexistence of gapless and gap excitations, which was originally discovered in doped spin-Peierls material $CuGeO_3$, was suggested in the ordered phase. Although the contribution from the Haldane-like gap excitation is small at low temperatures, it increases with temperature.

(b) Another possible source of the error may come from the subtraction of lattice heat capacity; the assumption that heat capacity in $PbMg_2V_2O_8$ is lattice heat capacity in $Pb(Ni_{1-x}M_x)_2V_2O_8$ might not be perfect.

Compared with the contribution of (a), that of (b) would be negligible in the temperature regions of Figs. 8, because the lattice heat capacity changes as $\sim T^3$. Hence we can simply assume that the magnetic entropy is the sum of contribution from the effective spin and spin-gap excitations, where the former is dominant in low temperature range and the latter is dominant in high temperature range. In Fig. 8 entropies with various Cu^{2+} concentration seem to converge near 12 K and simultaneously the entropies with low Cu^{2+} concentration have a point of inflection near the same temperature. Considering that the spin gap in $PbNi_2V_2O_8$ is about 20 K, the above experimental facts suggest the saturation of the entropy due to impurity-induced effective spins and the onset of contribution from the spin-gap excitation near

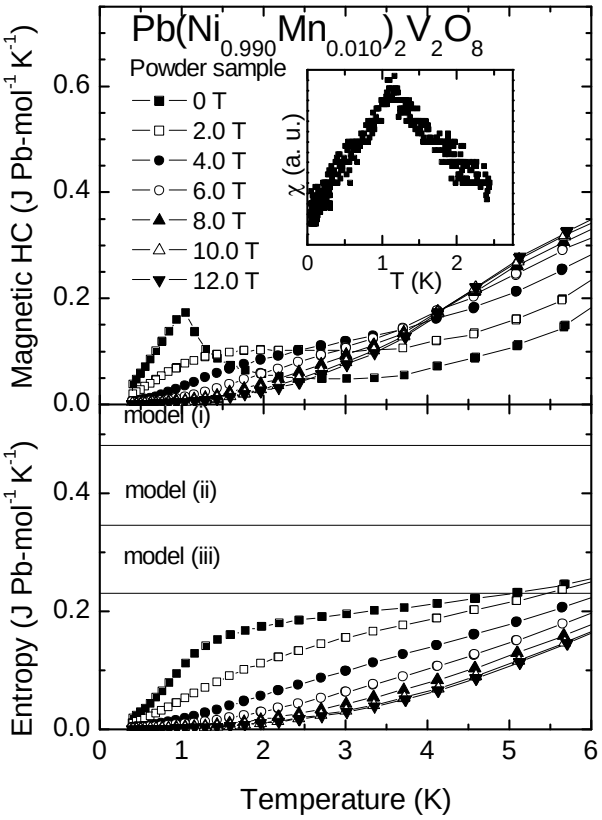

FIG. 9: Magnetic heat capacity (upper panel) and magnetic entropy (lower panel) of $Pb(Ni_{1-x}Mn_x)_2V_2O_8$ with $x = 0.010$. The inset shows AC susceptibility in the same sample measured in the adiabatic demagnetization refrigerator.

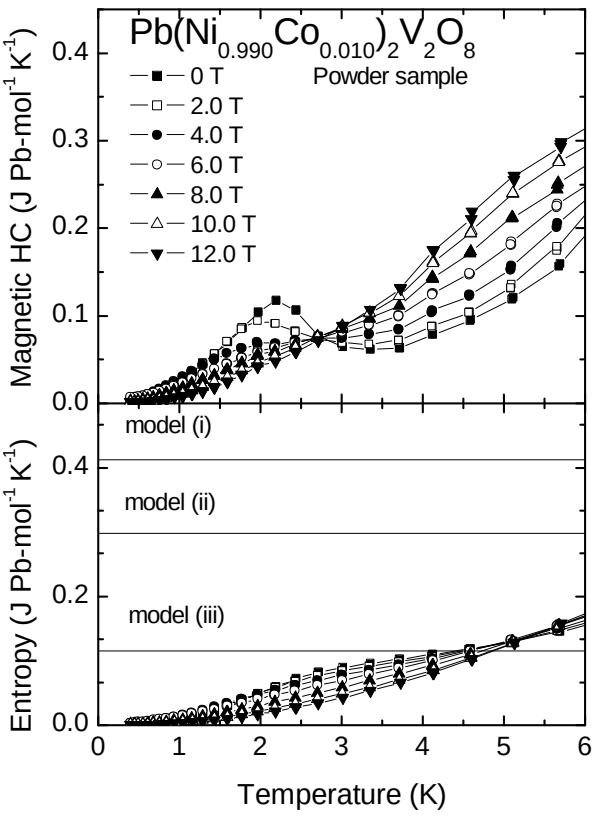

FIG. 10: Magnetic heat capacity (upper panel) and magnetic entropy (lower panel) of $Pb(Ni_{1-x}Co_x)_2V_2O_8$ with $x = 0.010$.

12 K. The experimental value of the entropy at $T \sim 12$ K is about 0.7 J Pb-mol^{-1}K^{-1} and this is the closest to the saturation entropy, $Nk_{\rm b}\ln(2\times\frac{1}{2}+1) = 0.576$ J Pb-mol^{-1}, calculated based on model (iii) proposed in the section III A. Hence, we conclude that two edge spins and the spin of impurity Cu^{2+} ion are *antiferromagnetically* coupled and one effective spin of $S = 1/2$ appears near the impurity spin. The conclusion is consistent with the argument in the section III A.

Magnetic heat capacities and magnetic entropies of $Pb(Ni_{1-x}Mn_x)_2V_2O_8$ with $x = 0.010$ and $Pb(Ni_{1-x}Co_x)_2V_2O_8$ with $x = 0.010$ are shown in Figs. 9 and 10, respectively. For Mn-doped sample, an anomaly due to the antiferromagnetic ordering is found in $H = 0$ T at 1.1 K, which is the same temperature of the anomaly in the AC susceptibility (see the inset). The anomaly disappeared above the magnetic field of $H = 2.0$ T. For $Pb(Ni_{1-x}Co_x)_2V_2O_8$ a broad peak of the magnetic heat capacity in zero magnetic field is observed at $T = 2.1$ K, which is the same temperature of the anomaly in the magnetic susceptibility (see Fig. 3 and the inset.) The weak ferromagnetism is concluded from both heat capacity and the magnetic susceptibility measurements. The anomaly is suppressed by the application of a magnetic field and disappears at $H = 4.0$ T.

Magnetic heat capacity and entropy in both $Pb(Ni_{1-x}Mn_x)_2V_2O_8$ and $Pb(Ni_{1-x}Co_x)_2V_2O_8$ are qualitatively the same as in $Pb(Ni_{1-x}Cu_x)_2V_2O_8$ and the similar argument leads to the same conclusion; the model (iii) proposed in the section III A is the best to describe the effective spin induced by impurities. J_M in the effective Hamiltonian in Eq. (4) is antiferromagnetic and one effective spin with $S = |S_M - 1|$ is detected in the magnetic-impurity-doped $PbNi_2V_2O_8$.

D. T–x phase diagram

T–x phase diagrams are *qualitatively* independent on the species of impurities as we can see in Fig. 11 . The transition temperatures increase with the impurity concentration and they reach their maximum at some concentrations. In higher concentration region the modest decreases are observed on $Pb(Ni_{1-x}M_x)_2V_2O_8$ ($M =$ Mg and Co) where the higher concentration samples are available. We find the similar feature of the T–x phase diagram in other spin-gap materials such as spin-Peierls

$CuGeO_3$,[21,22,23] two-leg spin ladder $SrCu_2O_3$,[24] and interacting dimer $TlCuCl_3$.[25] This shows that the phenomenon, i.e., impurity-induced antiferromagnetic long-range order in spin-gap materials, is universal as already discussed briefly in Refs. 10, 26, 27 and 28.

We find another common feature in the lightly-doped region. Small amount of impurities induce antiferromagnetic long-range order and the transition temperature does not decrease drastically in log-log scale, which is shown in Fig. 11 (b), and this suggests no threshold concentration in $Pb(Ni_{1-x}M_x)_2V_2O_8$. The absence of the threshold was also reported in Zn-doped $CuGeO_3$ by Manabe *et al.*[29] They studied the T–x phase diagram in low-concentration region and showed that the relation

$$T_{\rm N} = A \exp\left(-\frac{B}{x}\right), \tag{6}$$

holds in very low-temperature ($T \lesssim 8 \times 0.8$ K) and low-concentration ($x \lesssim 5 \times 10^{-3}$) region.

The unique feature in $Pb(Ni_{1-x}M_x)_2V_2O_8$ is that the transition temperatures drastically depend on the species of the impurities. The maximum transition temperature of $Pb(Ni_{1-x}Co_x)_2V_2O_8$ is more than 10 K, while that of $Pb(Ni_{1-x}Cu_x)_2V_2O_8$ is less than 1 K. Non-magnetic impurity Mg^{2+} induces lower transition temperature than Co^{2+} but, somehow, higher temperature than Mn^{2+} or Cu^{2+}. The seemingly mysterious behavior can be explained by considering effective Hamiltonian in Eqs. (3) and (4). The impurity dependence of the transition temperatures will be *semiquantitatively* discussed in the following section.

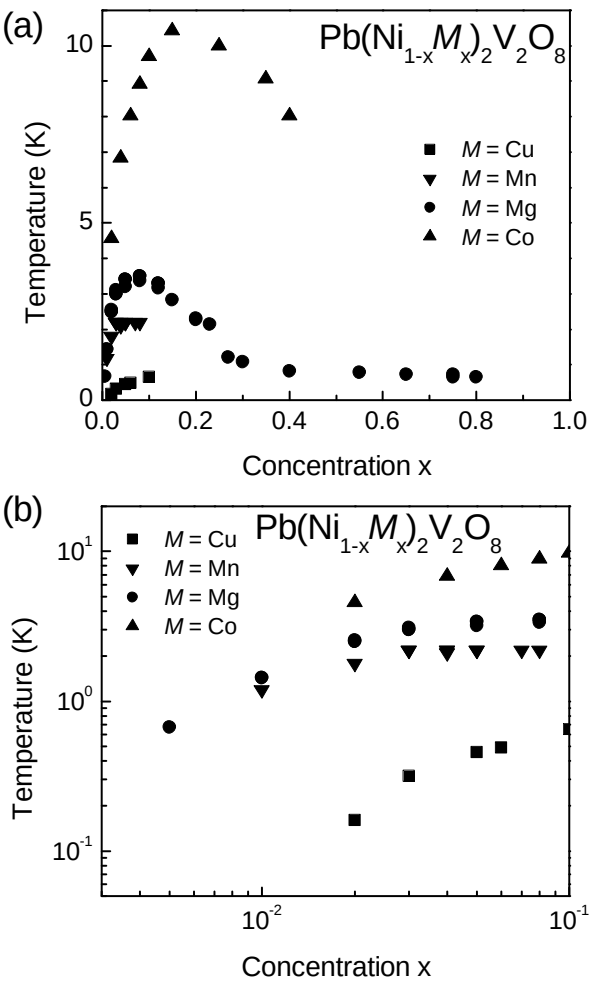

FIG. 11: (a) Temperature vs impurity concentration (T–x) phase diagram in impurity-doped Haldane material $PbNi_2V_2O_8$. (b) T–x phase diagram in the lightly doped region, where the data are plotted in log-log scales.

IV. DISCUSSION

The low-temperature phase of $Pb(Ni_{1-x}Co_x)_2V_2O_8$ showed a hysteresis in the susceptibility vs temperature curve and it was not a simple antiferromagnetic phase. The low-temperature phase of $Pb(Ni_{1-x}Co_x)_2V_2O_8$ can be attributed to the weak-ferromagnetic phase. The reason for the occurrence of the weak-ferromagnetic phase is due to the structure of $PbNi_2V_2O_8$, where the Ni chain (spin chain) is constructed as the four-fold screw chain.[30] The screw chain does not have an inversion center between the neighboring Ni sites and therefore the Dzyaloshinskii-Moriya (DM) interaction[19,20] exists between the two neighboring spins. As is well known, DM interaction can cause canting of the sublattice magnetization of the antiferromagnetic phase and the state becomes weak-ferromagnetic phase.

In Fig. 11 we see that the transition temperatures of $Pb(Ni_{1-x}M_x)_2V_2O_8$ differ much depending on the kind of impurities M even though the qualitative behavior is independent. The transition temperature is obtained as the divergence of the staggered susceptibility but there is no theoretical calculation for our specific case. However, it is possible to *semiquantitatively* explain the T–x phase diagram such as extremely low transition temperature in $Pb(Ni_{1-x}Cu_x)_2V_2O_8$ and very high transition temperature in $Pb(Ni_{1-x}Co_x)_2V_2O_8$.

As was already mentioned, the low energy excitation in the disordered state in a doped-Haldane chain is well explained by the effective Hamiltonian in Eq. (2). For the appearance of the ordered state in coupled-Haldane chains, on the other hand, the interchain interaction must be considered in addition. However, the consideration of the effective Hamiltonian Eq. (2) which includes only $J_{\rm NNN}$ and J_M would still be meaningful if we assume that impurity doping does not affect the interchain interaction. We could discuss the transition temperatures in $PbNi_2V_2O_8$ doped with various impurities by calculating the ground state energy in effective Hamiltonian Eqs. (3) and (4), and also by calculating the energy in local collinear spin structure; parallel in Fig. 1 (b) or antiparallel in Fig. 1 (c).

Firstly let us examine why $Pb(Ni_{1-x}Cu_x)_2V_2O_8$ or $Pb(Ni_{1-x}Mn_x)_2V_2O_8$ has lower transition temperatures than $Pb(Ni_{1-x}Mg_x)_2V_2O_8$. Effective Hamiltonian for $Pb(Ni_{1-x}Mg_x)_2V_2O_8$ is Eq. (3) and the ground state is ferromagnetic triplet state, as is visualized in Fig. 1(b). Such a collinear state conserves the coherence of antiferromagnetic correlation in the chain around the impurities. Hence three-dimensionally ordered state is favored by the local inchain interaction, ferromagnetic $J_{\rm NNN}$, as well as interchain interaction. On the other hand the effective Hamiltonian for $Pb(Ni_{1-x}Cu_x)_2V_2O_8$ or $Pb(Ni_{1-x}Mn_x)_2V_2O_8$ is expressed by Eq. (4). The local antiparallel spin structure (see Fig. 1 (c)), which favors coherence of antiferromagnetic correlation in the chain, is neither the ground state nor an eigenstate of the effective Hamiltonian. This means that the three-dimensionally ordered state in $Pb(Ni_{1-x}Cu_x)_2V_2O_8$ or $Pb(Ni_{1-x}Mn_x)_2V_2O_8$ is favored by interchain interaction but it is disturbed by the local inchain interaction, J_M. Therefore $Pb(Ni_{1-x}Cu_x)_2V_2O_8$ or $Pb(Ni_{1-x}Mn_x)_2V_2O_8$ has lower transition temperatures than $Pb(Ni_{1-x}Mg_x)_2V_2O_8$.

Secondly let us discuss the transition temperatures in $Pb(Ni_{1-x}Cu_x)_2V_2O_8$ and $Pb(Ni_{1-x}Mn_x)_2V_2O_8$. The ground states of both of the effective Hamiltonians are not a collinear spin state. This fact does not favor the antiferromagnetic coherence in the isolated chain and the appearance of ordered state is the result of the reduction in the energy of the ordered state due to the interchain interaction. In this case the transition temperature may be mainly determined by the energy difference between the ground state of the effective Hamiltonian and collinear spin state. We define

$$\Delta E_{M={\rm Cu,Mn}} \equiv \Big(\frac{E_{\rm collinear}-E_{\rm G}}{J_M s_1 S_M}\Big)_{M={\rm Cu,Mn}}, \qquad (7)$$

where

$$\begin{aligned} E_{{\rm collinear},M} &= \langle {\rm collinear}, M|\mathcal{H}_2|{\rm collinear}, M\rangle \\ |{\rm collinear}, M\rangle &= |s_1^z=1/2, S_M^z=-S_M, s_2^z=1/2\rangle. \end{aligned} \qquad (8)$$

For the appearance of three-dimensionally ordered state, large ΔE_M requires large energy reduction in the ordered state and this results in the lower transition temperature. The maximum transition temperatures $T_{\rm N}^{\rm max}$, $E_{{\rm G},M}$, $E_{{\rm collinear},M}$, and ΔE_M are summarized in Table I. We find $\Delta E_{\rm Cu} > \Delta E_{\rm Mn}$ and this is consistent with lower transition temperature in $Pb(Ni_{1-x}Cu_x)_2V_2O_8$ than in $Pb(Ni_{1-x}Mn_x)_2V_2O_8$.

Thirdly let us discuss the highest transition temperatures in $Pb(Ni_{1-x}Co_x)_2V_2O_8$. Since we have already explained that $Pb(Ni_{1-x}Mg_x)_2V_2O_8$ has the highest transition temperature among Mg-, Cu-, and Mn-doped $PbNi_2V_2O_8$, the comparison between $Pb(Ni_{1-x}Co_x)_2V_2O_8$ and $Pb(Ni_{1-x}Mg_x)_2V_2O_8$ is enough. So far we assumed implicitly that the spin interactions are isotropic. In some magnetic ions such as Co^{2+}, however, the interaction is possibly Ising-like because of remnant orbital momentum. In this case the first and the second term in Eq. (4) are modified;

$$\mathcal{H}_3 = J_{\rm Co}(s_1^z\cdot S_{\rm Co}^z + S_{\rm Co}^z\cdot s_2^z) + J_{\rm NNN}\boldsymbol{s}_1\cdot\boldsymbol{s}_2. \qquad (9)$$

The ground state of the effective Hamiltonian is spin collinear structure, as is similar to $Pb(Ni_{1-x}Mg_x)_2V_2O_8$, and the lower the ground state energy is, the higher the transition temperature will be. Useful physical quantities for $Pb(Ni_{1-x}Mg_x)_2V_2O_8$ and $Pb(Ni_{1-x}Co_x)_2V_2O_8$ are summarized in Table I. The ground state energy in $Pb(Ni_{1-x}Co_x)_2V_2O_8$ is lower than that of $Pb(Ni_{1-x}Mg_x)_2V_2O_8$ by $-(3/2)J_{\rm Co}$ and, therefore, the former has higher transition temperature. This means that $Pb(Ni_{1-x}Co_x)_2V_2O_8$ has the highest transition temperature.

The T–x phase diagram in $Pb(Ni_{1-x}M_x)_2V_2O_8$ has been *semiquantitatively* explained by the simple effective Hamiltonians based on VBS model. The drastic difference between magnetic impurity (Cu^{2+} or Mn^{2+}) and non-magnetic impurity (Mg^{2+}) is due to the different ground states. The highest transition temperature in $Pb(Ni_{1-x}Co_x)_2V_2O_8$ could be ascribed to Ising-type interaction. The effective Hamiltonians were successfully applied to Haldane materials but they can not be applied to other spin-gap materials such as $S=1/2$ spin-Peierls $CuGeO_3$. Indeed there is no drastic difference in the transition temperatures between non-magnetic impurity (Mg^{2+} or Zn^{2+}) and magnetic (Ni^{2+} $S=1$) impurity-doped $CuGeO_3$.[31]

In doped $CuGeO_3$ some of the present authors found that there is a first-order phase transition between the two kinds of antiferromagnetic phases with the change of the concentration of non-magnetic impurity Mg^{2+} (Refs. 22 and 23) or Zn^{2+}.[23] Two phases are the dimerized-antiferromagnetic (DAF) phase and uniform-antiferromagnetic (UAF) phase.[22] This phenomenon has been studied in detail by the various methods; thermal conductivity,[32] Raman scattering,[33] neutron diffraction,[34,35,36] pressure effect,[37,38,39] ESR,[40] and synchrotron x-ray scattering.[41] In Fig. 11(a) we see that the antiferromagnetic phase of $Pb(Ni_{1-x}Mg_x)_2V_2O_8$ extends very widely to $x\sim 1$ ($PbMg_2V_2O_8$ is not magnetic) and there seems no compositional phase transition in this wide region. On the contrary in Mg-doped $CuGeO_3$ the concentration region of the antiferromagnetic phase is more limited and there is a first-order compositional phase transition as mentioned above. The concept of the "impurity-induced antiferromagnetic phase" may only be applied to the lightly doped region in $Pb(Ni_{1-x}Mg_x)_2V_2O_8$. When the concentration x of Mg is very large, magnetic Ni^{2+} ions are randomly distributed three dimensionally among the non-magnetic Mg^{2+} ions and the ordered state may be constructed among these diluted Ni^{2+} spins. In $CuGeO_3$ the spin-gap state is caused by the spin-lattice interaction. In $CuGeO_3$ and doped $CuGeO_3$ spin gap is created by the spin-Peierls transition and the antiferromagnetic phase in the low impurity concentration region (DAF phase) has two order parameters: dimerization and antiferromag-

TABLE I: Summary of the maximum transition temperature, the ground state energy, collinear spin state energy, and the scaled energy difference. Details are explained in the text.

	M = Cu	M = Mn	M = Mg	M = Co
$T_{\rm N}^{\rm max}$	0.65 K ($x = 0.1$)	2.2 K ($x = 0.05$)	3.5 K ($x = 0.08$)	10.4 K ($x = 0.15$)
$\mathcal{H}$	$\mathcal{H}_2$	$\mathcal{H}_2$	$\mathcal{H}_1$	$\mathcal{H}_3$
$E_{{\rm G},M}$	$-J_{\rm Cu} + 1/4J_{\rm NNN}$	$-7/2J_{\rm Mn} + 1/4J_{\rm NNN}$	$1/4J_{\rm NNN}$	$-3/2J_{\rm Co} + 1/4J_{\rm NNN}$
$E_{{\rm collinear},M}$	$-1/2J_{\rm Cu} + 1/4J_{\rm NNN}$	$-5/2J_{\rm Mn} + 1/4J_{\rm NNN}$	$1/4J_{\rm NNN}$	$-3/2J_{\rm Co} + 1/4J_{\rm NNN}$
ΔE_M	2	4/5	0	0

netic long-range order. The difference of DAF and UAF phases in doped $CuGeO_3$ is the existence or absence of the lattice distortion (dimerization). On the contrary in $PbNi_2V_2O_8$ the spin gap is intrinsic and in the impurity-induced antiferromagnetic phase there is ony one order parameter (antiferromagnetic long-range order). The difference of the numbers of the order parameters may cause the different behavior of the compositional change between $Cu_{1-x}Mg_xGeO_3$ and $Pb(Ni_{1-x}Mg_x)_2V_2O_8$.

V. SUMMARY

Impurity-induced three-dimensional ordering is systematically studied in doped Haldane material $PbNi_2V_2O_8$ by use of DC and AC magnetic susceptibility, and heat capacity, on many samples with various species of impurities and concentrations. Complete T–x phase diagrams are obtained for each impurity and qualitatively common features to the doped spin-gap materials are observed. The unique feature is found in the drastic dependence of the transition temperatures on the species of the impurity, which is explained by effective Hamiltonian based on VBS model.

Acknowledgments

This work was partially supported by Grant-in-Aid for COE Research "SCP Project" from the Ministry of Education, Culture, Sports, Science, and Technology of Japan. One of the authors (T. M.) was partially supported by DOE Contract No. DE-AC05-00OR22725.

* Electronic address: imai.suguru@furukawa.co.jp. Present address: The Furukawa Electric Co., Ltd. 2-4-3 Okano, Nishi-ku, Yokohama 220-0073, Japan

† Electronic address: masudat@ornl.gov Present address: Condensed Matter Sciences Division, Oak Ridge National Laboratory, Oak Ridge, Tennessee 37831-6393, USA

‡ Present address: System Infrastructure Technologies, System Research & Development Center, NS Solutions Corporation, 3-3-1, Minatomirai, Nishi-ku, Yokohama 220-8401, Japan

§ Present address: The Institute of Physical and Chemical Research (RIKEN), Wako, Saitama 351-0198, Japan

[1] H. Bethe, Z. Phys. **71**, 205 (1931).

[2] J. des Cloizeaux and J. J. Pearson, Phys. Rev. **128**, 2131 (1962).

[3] F. D. M. Haldane, Phys. Lett. **93A**, 464 (1983).

[4] F. D. M. Haldane, Phys. Rev. Lett. **50**, 1153 (1983).

[5] I. Affleck, T. Kennedy, E. H. Lieb, and H. Tasaki, Phys. Rev. Lett. **59**, 799 (1987).

[6] I. Affleck, T. Kennedy, E. H. Lieb, and H. Tasaki, Commun. Math. Phys. **115**, 477 (1988).

[7] M. Hagiwara, K. Katsumata, I. Affleck, B. I. Halperin, and J. P. Renard, Phys. Rev. Lett. **65**, 3181 (1990).

[8] T. Kennedy, J. Phys.: Cond. Matter **2**, 5737 (1990).

[9] S. Miyashita and S. Yamamoto, Phys. Rev. B **48**, 913 (1993).

[10] Y. Uchiyama, Y. Sasago, I. Tsukada, K. Uchinokura, A. Zheludev, T. Hayashi, N. Miura, and P. Böni, Phys. Rev. Lett. **83**, 632 (1999).

[11] A. Zheludev, T. Masuda, I. Tsukada, Y. Uchiyama, K. Uchinokura, P. Böni, and S. H. Lee, Phys. Rev. B **62**, 8921 (2000).

[12] K. Uchinokura, Y. Uchiyama, T. Masuda, Y. Sasago, I. Tsukada, A. Zheludev, T. Hayashi, N. Miura, and P. Böni, Physica B **284-288**, 1641 (2000).

[13] A. Zheludev, T. Masuda, K. Uchinokura, and S. E. Nagler, Phys. Rev. B **64**, 134415 (2001).

[14] A. Zorko, D. Arčon, A. Lappas, J. Giapintzakis, C. Saylor, and L. C. Brunel, Phys. Rev. B **65**, 144449 (2002).

[15] T. Masuda, K. Uchinokura, T. Hayashi, and N. Miura, Phys. Rev. B **66**, 174416 (2002).

[16] N. D. Mermin and H. Wagner, Phys. Rev. Lett. **17**, 1133 (1966).

[17] A. I. Smirnov, V. N. Glazkov, H. A. Krug von Nidda, A. Loidl, L. N. Demianets, and A. Y. Shapiro, Phys. Rev. B **65**, 174422 (2002).

[18] K. Uchinokura, T. Masuda, Y. Uchiyama, and R. Kuroda, J. Mag. Mag. Mater. **226-230**, 431 (2001).

[19] I. Dzyaloshinskii, Soviet Phys.-JETP **5**, 1259 (1957).

[20] T. Moriya, Phys. Rev. **120**, 91 (1960).

[21] N. Koide, Y. Sasago, T. Masuda, and K. Uchinokura, Czech. J. Phys. **46(S2)**, 1981 (1996).

[22] T. Masuda, A. Fujioka, Y. Uchiyama, I. Tsukada, and K. Uchinokura, Phys. Rev. Lett. **80**, 4566 (1998).

[23] T. Masuda, I. Tsukada, K. Uchinokura, Y. J. Wang, V. Kiryukhin, and R. J. Birgeneau, Phys. Rev. B **61**, 4103 (2000).

[24] M. Azuma, Y. Fujishiro, M. Takano, M. Nohara, and

H. Takagi, Phys. Rev. B **55**, R8658 (1997).
[25] A. Oosawa, T. Ono, and H. Tanaka, Phys. Rev. B **66**, 020405 (2002).
[26] K. Uchinokura and T. Masuda, J. Phys. Soc. Jpn. **69 Suppl. A**, 287 (2000).
[27] K. Uchinokura, J. Phys.: Cond. Matter **14**, R195 (2002).
[28] K. Uchinokura, Prog. Theor. Phys. Suppl. **145**, 294 (2002).
[29] K. Manabe, H. Ishimoto, N. Koide, Y. Sasago, and K. Uchinokura, Phys. Rev. B **58**, R575 (1998).
[30] R. Wichmann and H. Müller-Buschbaum, Rev. Chim. Miner. **23**, 1 (1986).
[31] T. Masuda, N. Koide, and K. Uchinokura, Prog. Theor. Phys. Suppl. **145**, 306 (2002).
[32] J. Takeya, I. Tsukada, Y. Ando, T. Masuda, and K. Uchinokura, Phys. Rev. B **61**, 14700 (2000).
[33] H. Kuroe, H. Seto, T. Sekine, T. Masuda, I. Tsukada, and K. Uchinokura, Physica B **263-264**, 825 (1999).
[34] H. Nakao, M. Nishi, Y. Fujii, T. Masuda, I. Tsukada, K. Uchinokura, K. Hirota, and G. Shirane, J. Phys. Chem. Solids **60**, 1117 (1999).
[35] H. Nakao, M. Nishi, Y. Fujii, T. Masuda, I. Tsukada, K. Uchinokura, K. Hirota, and G. Shirane, J. Phys. Soc. Jpn **68**, 3662 (1999).
[36] M. Nishi, H. Nakao, Y. Fujii, T. Masuda, K. Uchinokura, and G. Shirane, J. Phys. Soc. Jpn **69**, 3186 (2000).
[37] T. Masuda, R. Kuroda, and K. Uchinokura, J. Mag. Mag. Mater. **226-230**, 425 (2001).
[38] Y. Tanokura, Y. Oono, S. Ikeda, H. Kuroe, T. Sekine, T. Masuda, and K. Uchinokura, Phys. Rev. B **68**, 054412 (2003).
[39] T. Masuda, D. Yano, R. Kuroda, K. Uchinokura, H. Kuroe, T. Sekine, Y. Katsuki, K. Ohwada, Y. Fujii, H. Nakano, et al., Phys. Rev. B **67**, 024423 (2003).
[40] V. N. Glazkov, A. I. Smirnov, K. Uchinokura, and T. Masuda, Phys. Rev. B **65**, 144427 (2002).
[41] Y. J. Wang, Y. J. Kim, R. J. Christianson, S. C. LaMarra, F. C. Chou, T. Masuda, I. Tsukada, K. Uchinokura, and R. J. Birgeneau, J. Phys. Soc. Jpn. **72**, 1544 (2003).